Emergency Management
Science and Technology

ARTICLE

Open Access

https://doi.org/10.48130/emst-0026-0007
Emergency Management Science and Technology **2026**, 6: e008

Study on reaction exothermic mechanism and hazard assessment for the synthesis of propylene glycol methyl ether (PGME) from propylene oxide (PO) and methanol

Xiaoyu Fang[1], Na Li[1], Lei Ni[1,2*], Zhen Cheng[1], Zhiquan Chen[1,2] and Zhiping Li[1]

[1] *College of Safety Science and Engineering, Nanjing Tech University, Nanjing 211816, China*
[2] *Jiangsu Key Laboratory of Hazardous Chemicals Safety and Control, Nanjing Tech University, Nanjing 211816, China*
* Correspondence: lei_ni@163.com (Ni L)

Abstract

Propylene glycol methyl ether, as an important solvent, releases a large amount of heat during its synthesis process and poses certain hazards. In this study, the reaction was carried out in a semi-batch mode. The parameter range for optimization was determined via single-factor experiments. The process parameters, including the reaction temperature, the alcohol-to-alkane ratio, and the catalyst concentration, were selected as the main factors to optimize the reaction yield and pressure by response surface methodology. The results showed that when the reaction temperature was 100 °C, the alcohol-to-alkane ratio was 4, and the catalyst concentration was 0.77%, the yield could reach the maximum of 88.58%, and the pressure decreased to 3.62 bar. The exothermic behavior of the synthesis of PGME was studied by calorimetric experiments. Simultaneously, density functional theory (DFT) was used to calculate the reaction pathway and thermal behavior of the reaction. The concentration changes of reactants and products were monitored by Fourier Transform InfraRed, in real time (FTIR). An adiabatic accelerated calorimeter was used to study the thermal stability of materials. Finally, the runaway risk of the reaction was evaluated based on the risk matrix method and the Stoessel critical diagram method. The results showed that the risk level of the reaction was level 3, and it also reveals the mechanism of heat release during the reaction, which can be used to guide the safe production of propylene glycol methyl ether.

Keywords: Propylene glycol methyl ether, Process optimization, Exothermic behavior, Online infrared, Reaction evaluation

Citation: Fang X, Li N, Ni L, Cheng Z, Chen Z, et al. 2026. Study on reaction exothermic mechanism and hazard assessment for the synthesis of propylene glycol methyl ether (PGME) from propylene oxide (PO) and methanol. *Emergency Management Science and Technology* 6: e008 https://doi.org/10.48130/emst-0026-0007

Introduction

The chemical industry involves a large amount of toxic, explosive, and other hazardous substances. Dangerous working conditions may arise during production processes. Once an accident occurs, the consequences are often devastating. Propylene glycol ethers are essential and widely used chemical products. Due to their two strong functional groups, the ether bond and the hydroxyl group, the ether bond is lipophilic and can dissolve hydrophobic substances, while the hydroxyl group is hydrophilic and can dissolve hydrophilic substances[1]. Due to their low toxicity[2,3], propylene glycol ethers have become widely used solvents. PGME is a colorless, transparent liquid and is one of the main products among propylene glycol ethers.

PGME can be synthesized from PO and methanol (MeOH) under the catalysis of a catalyst[4]. The early BF3 catalyst[5] had strong corrosivity to equipment, caused serious pollution, and resulted in poor product selectivity and low yield. Subsequently, many alkaline catalysts were developed. Timofeeva et al.[6] studied the effect of the zeolitic imidazolate framework (ZIF-8) and its composite, with alumina nanofibers as heterogeneous catalysts, on the yield of PGME, proposing that as the ZIF-8 crystal size increases, both the reaction rate and selectivity to PGME decrease. Zhao et al.[7] prepared acetate ionic liquids for catalyzing the reaction of PO with alcohol to synthesize propylene glycol ether. Compared to traditional sodium hydroxide catalysts, it effectively reduces the formation of by-products. The catalytic performance improves with increasing catalyst concentration. In this system, the optimal molar ratio of alcohol to PO is approximately 3, and the optimal temperature is around 140 °C. Timofeeva et al.[8] studied the activity mechanism, shape selectivity, and stability of alumina pillared interlayer clay (Al-PILC) in catalyzing the ring-opening etherification reaction of methanol and PO. The optimal reaction conditions were obtained as follows: temperature of 110 °C, molar ratio of methanol to PO of 10, catalyst dosage of 3 wt%, and a reaction time of 2 h. Currently, potassium hydroxide and sodium hydroxide are mainly used as catalysts for the synthesis of propylene glycol ethers in industry, mainly due to the easy availability of the catalysts and the considerable yield.

The synthesis of propylene glycol ethers from PO and alcohols is highly exothermic and rapid, presenting significant safety hazards. Additionally, epoxides generally have high heat of polymerization, with PO having a heat of polymerization of 83 kJ/mol and ethylene oxide having a heat of polymerization of 95 kJ/mol[9]. Polymerization reactions are mostly carried out under high temperature and high pressure conditions, and many of the catalysts, reactants, initiators, etc., used in these reactions are flammable and explosive[10,11]. Taking PO as an example, its boiling point is only 34 °C, and its flash point is −37.2 °C, making it prone to explosion accidents.

The study of thermal hazards associated with reactions has always been a hot topic. Bou-diab & Fierz[12] developed a dynamic DSC measurement screening method to identify autocatalytic decomposition. By fitting a first-order kinetic model to the measured exothermic curve, 80% of autocatalytic reactions can be identified. Stoessel et al.[13], through the summary and research of numerous

https://doi.org/10.48130/emst-0026-0007

hazardous cases, developed the Stoessel analysis method and established a reaction hazard rating system, which is widely used in many industrial productions. Xu et al.[14] utilized the Stoessel analysis method to conduct a reaction risk assessment for the reaction process of diazidoacetaldoxime (DAzG). Combining a reaction calorimeter and an accelerated adiabatic calorimeter, he ultimately classified the exothermic risk of DAzG as Level 2. Jiang et al.[15] proposed an improved method for the Stoessel critical diagram, incorporating the final temperature under adiabatic conditions into the thermal hazard assessment. Based on the improved Stoessel critical diagram, he evaluated the synthesis of tert-butyl peroxyacetate, the preparation of hydroxylamine, and the synthesis of 2,6-diethyl-4-methylphenylpropanamide, obtaining evaluation results that were more in line with reality. Berdouzi et al.[16] developed a process safety method based on the HAZOP classical framework, combining dynamic simulation of deviation scenarios and risk matrix tools. This method can quantify the impact of deviations and can be applied in complex process patterns. Wang et al.[17] conducted experiments on benzaldehyde oxime (BO) using DSC, performed linear fitting on the decomposition kinetics of BO, and simulated the thermal behavior under isothermal, adiabatic, and finite heat transfer conditions. The simulation results showed that BO decomposes in the liquid phase and releases a large amount of energy. Meanwhile, the effective activation energy range of BO was measured to be 68.9 to 41.3 kJ/mol, confirming that the decomposition of BO is a multi-step reaction. Yu et al.[18] studied the polymerization process of styrene, deriving the thermal runaway criterion for styrene polymerization through calorimetric experiments and gas chromatography experiments. It was demonstrated that the hazard of styrene polymerization increases with rising temperature, and the adiabatic temperature rise of the reaction increases logarithmically. Chen et al.[19] studied the exothermic behavior of the decomposition of cumene hydroperoxide (CHP), used the obtained data to simulate the runaway behavior of 88% mass fraction CHP, developed a simplified self-heating rate equation, and found that the presence of metal ions in CHP significantly increases the risk of runaway.

The synthesis of PGME involves the ring-opening addition of PO. Due to the physicochemical properties of PO and MeOH, the reaction is highly exothermic and often conducted under pressure. If cooling fails during production[20], the heat generated by the reaction will accelerate the process, leading to an explosion.

This work investigates the exothermic characteristics of the synthesis of PGME from PO. PO and MeOH are used as reactants, with KOH serving as the catalyst, and the synthesis is conducted in semi-batch mode. A single-factor experiment design is employed to evaluate the effects of reaction temperature (T_p), catalyst concentration, alcohol-to-alkane ratio, and feeding rate on product yield and maximum system pressure. Based on these results, optimal parameters are selected, and the process is further optimized using a three-factor, three-level design method based on response surface methodology (RSM). Additionally, the exothermic behavior of the reaction under varying conditions is examined. Changes in reactant concentration and heat release during the reaction process are monitored using an online infrared detector. The experimental products are characterized and analyzed using adiabatic calorimetry. Finally, the hazard level of the reaction is assessed using the risk matrix method and the Stossel critical diagram. The reaction equation is presented in Fig. 1.

Chemicals and methods

Chemicals

The chemicals used in this experiment are listed in Table 1.

Experimental design

Single-factor experiments

Before conducting process optimization, in order to better observe the effects of reaction temperature, catalyst concentration, alcohol-to-alkane ratio, and feeding rate on product yield and pressure, a single-factor experiment is required. Control experiments, as described in Table 2, have been designed.

Process optimization

In this work, the main focus was on optimizing the process through experimental design. Using the Box-Behnken method in Design-Expert software, appropriate parameters and ranges for optimization experiments were determined based on the single-factor experimental results presented in Table 3. The results indicated that the feeding rate had a minor impact on yield but a significant effect on system pressure, whereas the alcohol-to-alkane ratio had a substantial influence on the yield but a minor effect on the system pressure. To achieve a higher yield, reaction temperature (X_1), catalyst concentration (X_2), and alcohol-to-alkane ratio (X_3) were selected as key parameters. Using the yield of PGME and system pressure as the response variables, a polynomial regression model was established to quantify the relationships between the input variables and the responses. The experimental factors and their levels are presented in Table 3.

Experimental apparatus and methods

Characterization experiment of reaction products

The reaction products were analyzed using a gas chromatograph (GC 7890B, Agilent Technologies, Inc.). A standard calibration curve was plotted using pure substances, and the yield was analyzed based on this curve. The gas chromatograph was equipped with a capillary column (HP-5, 30 m × 0.32 mm × 0.25 μm) and a flame ionization detector (FID). The sample injection volume was 1μL per injection, and the injector temperature was set to 290 °C. The oven temperature was initially held at 60 °C for 2 min, then increased to 140 °C at a rate of 10 °C/min and maintained for 2 min. The entire process was carried out under a nitrogen atmosphere with a flow rate of 1.5 mL/min, using hydrogen and synthetic air as the detector gases for flame ionization[21].

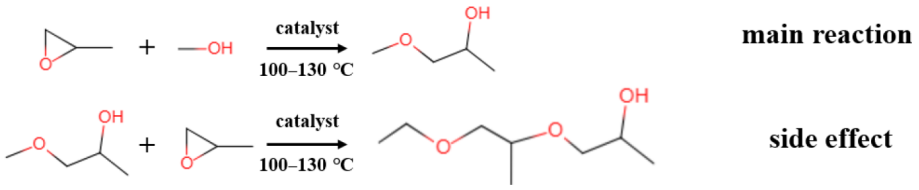

Fig. 1 Synthesis of propylene glycol monomethyl ether and side reaction equation.

Table 1. Chemicals used in the experiment.

Chemical	CAS No.	Molecular formula	Purity (%)	Source
MeOH	67-56-1	CH_4O	99.9	Aladdin
PO	75-56-9	C_3H_6O	99.5	Macklin
KOH	1310-58-3	KOH	90	Sinopharm
n-hexane	110-54-3	C_6H_{14}	99	Macklin
PGME	107-98-2	$C_4H_{10}O_2$	99	Macklin

Table 2. Single-factor controlled experimental group design.

Experimental group	Reaction temperature (°C)	Catalyst concentration (%)	Alcohol-to-alkane ratio	Feeding rate (mL/min)
a	100	0.5	3	20
	110	0.5	3	20
	120	0.5	3	20
	130	0.5	3	20
b	100	1	2	20
	100	1	3	20
	100	1	4	20
	100	1	5	20
c	100	0.5	3	20
	100	1	3	20
	100	1.5	3	20
	100	2	3	20
d	120	1	4	20
	120	1	4	30
	120	1	4	40

The catalyst concentration is expressed as a percentage of the total mass.

Table 3. Box-Behnken experimental design.

Factors	Symbol	Levels		
		−1	0	1
T_r (°C)	X_1	100	110	120
Catalyst concentration (%)	X_2	0.5	1	1.5
Alcohol-to-alkane ratio	X_3	2	3	4

Theoretical calculation

To study the reaction mechanism of this reaction, the quantum chemistry software Gaussian was used. Under the theoretical framework of density functional theory with the B3LYP method and 6−311 G (d,p) basis set, the geometric optimization and vibrational frequency calculation of the reactant (R) and product (P) in the reaction system were carried out to find the most stable structure with the lowest energy in the reaction system. Subsequently, the single-point energy was calculated at the theoretical level of the B3LYP method and def2TZVPP basis set, and the reaction path and reaction enthalpy during the process were obtained. These were then used to calculate the heat of reaction.

Reaction process monitoring experiment

In this work, an online infrared spectrometer (ReactIRTM 15) was used to monitor the process by analyzing changes in peak intensities, thereby inferring variations in the composition of the reaction system. The wavenumber range was set from 650 to 3,000 cm^{-1} during the experiments[22]. The probe was inserted into the autoclave through an adapter and submerged below the liquid surface, with scans and data recorded every 15 s.

Calorimetry experiment

In this work, a fully automated reaction calorimeter (RC1e, Mettler Toledo, Switzerland) was used to study the exothermic characteristics of the reaction[23]. The heat of the entire system includes q_{ac}, q_{flow}, q_{dos}, q_{loss}, and q_c, while the exothermic rate of the reaction, q_r, is described in the energy conservation Eq. (1).

$$q_r = q_{ac} + q_{flow} + q_{dos} + q_{loss} - q_c \quad (1)$$

q_r represents the heat release rate, W. The heat release rate of the entire reaction is composed of the above five types of heat, calculated through the loss and accumulated heat. q_{ac} is the accumulated heat, W; q_{flow} is the heat transfer rate between the reaction vessel and the jacket, W; q_{dos} is the latent heat caused by the feeding process, W; q_{loss} is the heat dissipated from the reaction system to the environment, W; and q_c is the calibration power, W.

The schematic diagram of the reaction device is shown in Fig. 2.

Thermal decomposition experiments

The thermal decomposition characteristics of the product were analyzed using an accelerated adiabatic calorimeter. The sample was weighed at 1 g and placed into a 10 mL stainless steel test ball, and the analysis was conducted in the heating-waiting-search (H-W-S) mode. The initial temperature was set at 40 °C, the final temperature at 350 °C, with an interval of 10 °C, and a dwell time of 10 min to measure the exothermic behavior. The temperature rise detection threshold during the entire experiment was set at 0.02 °C/min.

The Stoessel critical diagram

The final hazard assessment of this reaction requires the use of the Stoessel critical graph method[13], which involves four parameters: process temperature (T_p), maximum temperature of the synthesis reaction (*MTSR*), temperature at 24 h of TMR_{ad} (T_{D24}), and maximum technical temperature (*MTT*). This method divides the process into five levels based on the comparison of the four parameters.

Results and discussion

Gas phase analysis

Qualitative analysis of substances

Diluted propylene glycol monomethyl ether and PO with *n*-hexane was used for gas chromatography testing. As shown in Fig. 3, the highest peak corresponds to the solvent. Near 3.06 and

Fig. 2 Schematic diagram of the reaction device.

https://doi.org/10.48130/emst-0026-0007

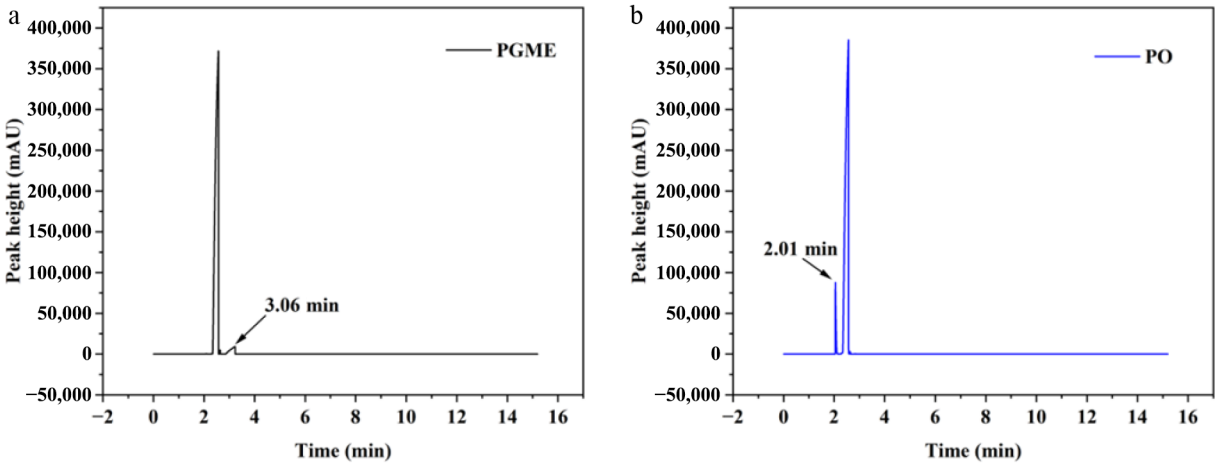

Fig. 3 Gas phase curves of propylene glycol monomethyl ether and PO solutions: (a) propylene glycol monomethyl ether solution, (b) PO solution.

2.01 min, peaks for propylene glycol monomethyl ether and PO are observed, respectively. By determining the peak times, a basis can be provided for subsequent drawing of working curves and analysis of products.

Quantitative analysis of substances

PGME and PO were diluted with *n*-hexane at concentrations of 0.1, 0.2, 0.3, 0.4, 0.5, 0.6, 0.7, 0.8, 0.9, and 1.0 (mass fraction), and gas chromatography tests were conducted on samples with different concentrations. The peak area (mAU·min) was plotted against the concentration on the *y*-axis and *x*-axis, respectively, to draw the working curve, as shown in Fig. 4. The correlation coefficient R^2 for the fitting of PGME was 0.9999, and that for PO was 0.9994, indicating good fitting results for both. The constructed linear function can be used to measure and calculate the amount of substance required in the product, and thus calculate the yield.

Theoretical calculation results

Figure 5 shows the reaction pathway of PO and methanol to form PGME, presenting the energy distribution of reactants, transition states, and reaction products. Under the conditions of 100 °C and 3 bar, the theoretical reaction enthalpy calculated is 85.41 kJ/mol, while the measured value after the reaction using RC1e under the same conditions is 84.95 kJ/mol, which is very close, verifying the reliability of the calculation.

Single-factor controlled experiment

Table 4 summarizes the effects of reaction temperature, catalyst concentration, alcohol-to-alkane ratio, and feeding rate on yield and maximum pressure in the reaction system. The results are shown in Fig. 6. No unreacted propylene oxide was detected in the experimental products, indicating that propylene oxide was completely consumed with a conversion rate of 100%. The reaction temperature exhibits a trend of first increasing and then decreasing within the range of 100–130 °C, and the same trend is observed when the catalyst concentration is between 0.5%–2.0%. However, as the feed rate decreases and the alcohol-to-alkane ratio increases, the yield continuously rises. An increase in reaction temperature, alcohol-to-alkane ratio, and feed rate will elevate the maximum pressure value of the reaction system, whereas an increase in catalyst concentration will reduce it. The purpose of process optimization is to obtain experimental parameters that yield optimal benefits and ensure a safe pressure environment for subsequent process optimization. The reaction temperature was selected as 100, 110, and 120 °C, and the catalyst concentration was chosen as 0.5%, 1%, and 1.5%. Since further increasing the alcohol-to-alkane ratio does not significantly benefit the yield and would result in methanol wastage, the ratios were set at 2, 3, and 4 with the feeding rate uniformly set at 20 mL/min.

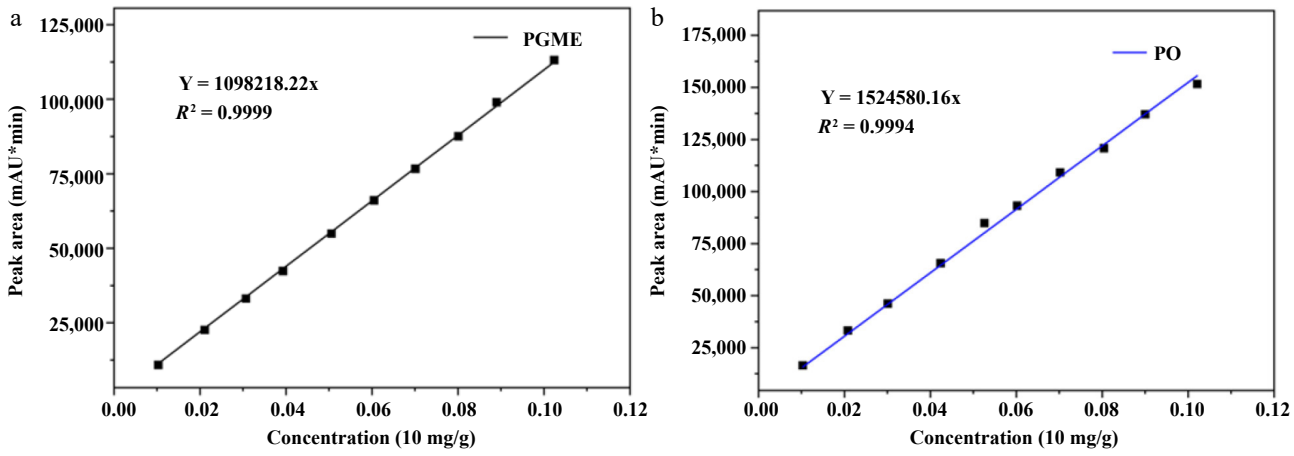

Fig. 4 (a) Standard curve of propylene glycol monomethyl ether; (b) standard curve of PO.

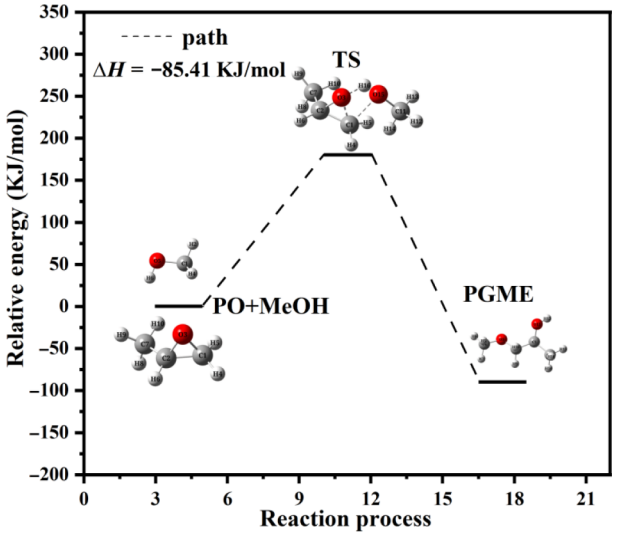

Fig. 5 Reaction pathways and enthalpy of reaction.

Table 4. Results of single-factor experiment.

Group	T_r (°C)	Catalyst concentration (%)	Alcohol-to-alkane ratio	Feeding rate (mL/min)	Yield (%)	P_{max} (bar)
a	100	0.5	3	20	85.47	3.7
	110	0.5	3	20	86.86	4.53
	120	0.5	3	20	82.27	6.02
	130	0.5	3	20	80.69	7.79
b	100	1	2	20	81.96	3.4
	100	1	3	20	85.26	3.41
	100	1	4	20	87.57	3.43
	100	1	5	20	88.98	3.47
c	100	0.5	3	20	85.47	3.7
	100	1	3	20	86.26	3.41
	100	1.5	3	20	82.45	3.38
	100	2	3	20	75.48	2.94
d	120	1	4	20	79.47	5.92
	120	1	4	30	79.06	6.23
	120	1	4	40	77.6	6.5

Process optimization

Model fitting

Table 5 summarizes the 17 experimental runs conducted to fit the model. According to the analysis of variance results, the *F* values for all three yield response variables are high, the overall model *p*-value is less than 0.0001, and the *F* value for the lack-of-fit term is 0.5895, which is not significant. These results indicate that the model is statistically significant and fits the data well. For the three pressure response variables, the *F* value for the X_3 is relatively low; however, the model remains significant, and the lack-of-fit *F* value is 0.7096, also not significant, confirming a good model fit.

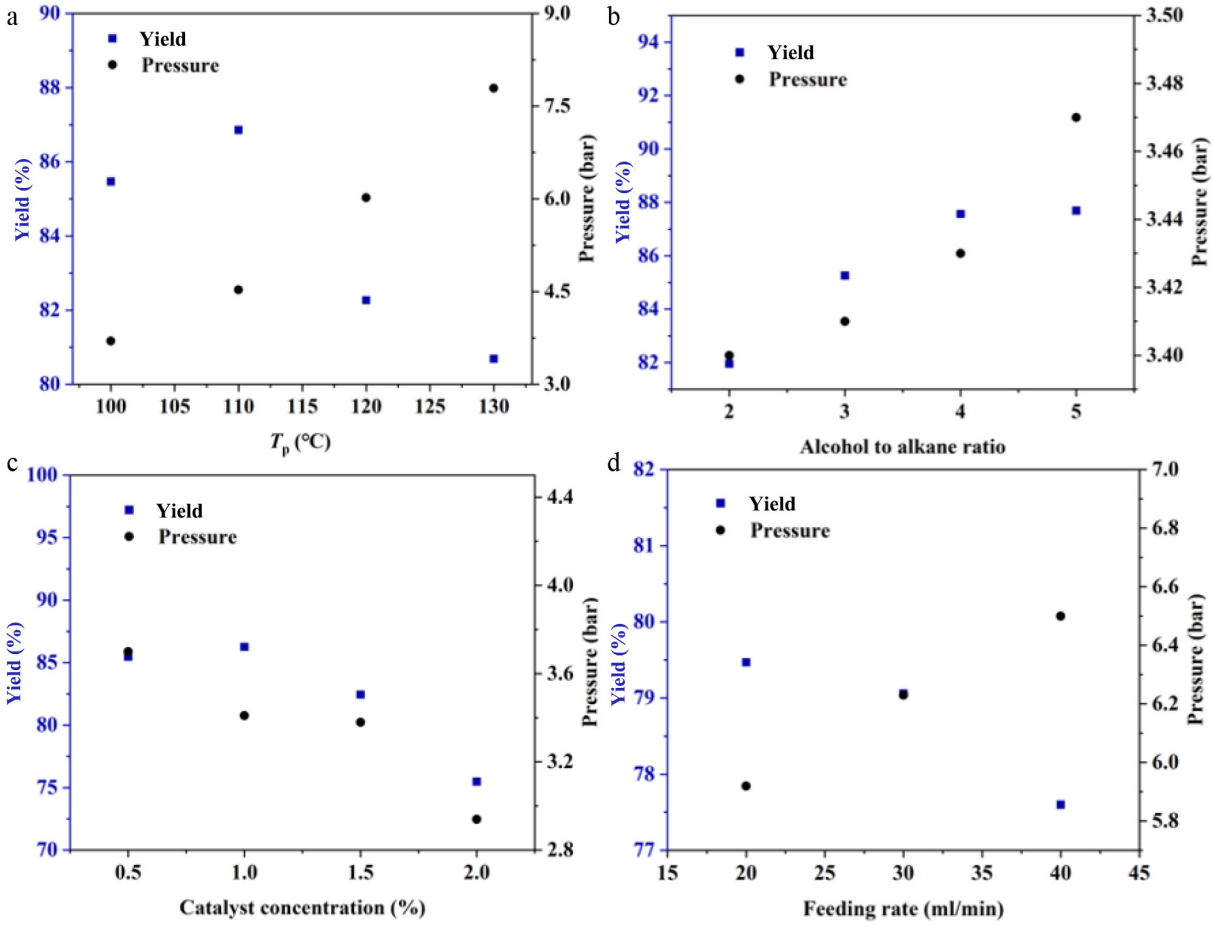

Fig. 6 The impact of various factors on yield and the maximum pressure of the system: (a) reaction temperature; (b) alcohol-to-alkane ratio; (c) catalyst concentration; (d) feeding rate.

https://doi.org/10.48130/emst-0026-0007

Table 5. Experimental results based on Box-Behnken.

Run	Independent variables			Dependent variables			
				Y_1		Y_2	
	X_1	X_2	X_3	Experimental value	Predictive value	Experimental value	Predictive value
1	110	1	3	86.12	86.12	4.41	4.47
2	110	1	3	87.36	87.36	4.54	4.47
3	120	1	2	83.72	83.72	5.88	5.84
4	110	0.5	2	84.94	84.94	4.56	4.57
5	110	1.5	4	84.32	84.32	4.43	4.42
6	110	1	3	86.24	86.24	4.49	4.47
7	100	0.5	3	85.47	85.47	3.70	3.68
8	100	1	2	81.96	81.96	3.40	3.41
9	120	0.5	3	82.27	82.27	6.02	6.05
10	100	1	4	87.57	87.57	3.43	3.47
11	110	1.5	2	83.43	83.43	4.36	4.38
12	120	1.5	3	80.06	80.06	5.87	5.89
13	110	0.5	4	86.95	86.95	4.68	4.66
14	110	1	3	86.58	86.58	4.40	4.47
15	110	1	3	86.43	86.43	4.53	4.47
16	100	1.5	3	82.45	82.45	3.41	3.39
17	120	1	4	79.47	79.47	5.92	5.91

Relationship between response variables and influencing factors

According to the results of variance analysis, regarding yield, besides the effects of reaction temperature, catalyst concentration, and alcohol-to-alkane ratio, it is also influenced by cross terms such as X_1X_2 and X_1X_3. The second-order polynomial of the encoded factors for the yield of propylene glycol monomethyl ether is shown in Eq. (2).

$$Y_1 = 86.55 - 1.49X_1 - 1.17X_2 - 2.47X_1X_3 - 2.86X_1^2 - 1.13X_2^2 \quad (2)$$

Regarding the maximum pressure of the system, it is most significantly influenced by X_1, while X_3 has a less significant impact. The second-order polynomial of the maximum pressure in terms of the coding factors is presented in Eq. (3).

$$Y_2 = 4.47 + 1.22X_1 - 0.1112X_2 + 0.213X_1^2 \quad (3)$$

As shown in Fig. 7, with increasing temperature and catalyst concentration, the yield first rises and then falls. This is because increasing temperature and catalyst concentration not only promote the main reaction, but also accelerate side reactions. When the reaction temperature becomes excessively high, the yield shows a downward trend. In contrast, increasing the alcohol-to-alkene ratio improves the yield. A higher ratio means a greater amount of methanol, which effectively reduces the chance of further contact

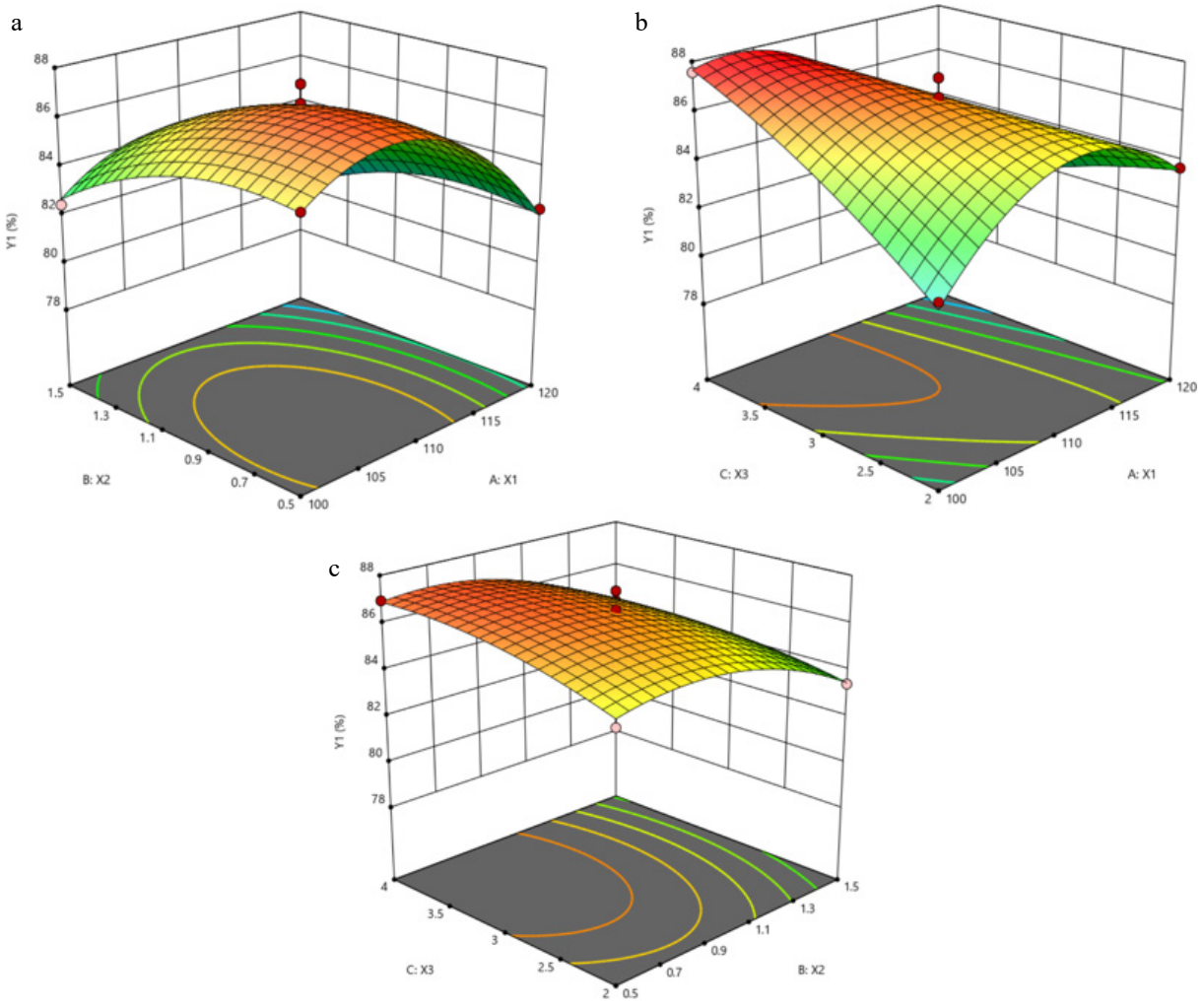

Fig. 7 Three-dimensional response plot of PGME yield: (a) X_1 and X_2; (b) X_1 and X_3; (c) X_2 and X_3.

between propylene oxide and propylene glycol monomethyl ether, thereby inhibiting the formation of the byproduct dipropylene glycol monomethyl ether. Therefore, in actual production, the reaction temperature and catalyst concentration should be properly controlled, and the alcohol-to-alkene ratio should be increased.

As shown in the three-dimensional response surface plot of the maximum pressure of the system depicted in Fig. 8, since the main reactants in this reaction are all low-boiling substances, the pressure increases continuously and more significantly with the rise of reaction temperature. Increasing the catalyst concentration can reduce the pressure because a higher catalyst concentration accelerates the reaction rate and achieves rapid consumption of propylene oxide, thus effectively lowering the system pressure.

Process optimization and result verification

Excessive pressure often leads to accidents. To identify the optimal process with higher yield and lower pressure expectations, the 'optimization' function in Design-Expert[24,25] software was utilized, with X_1, X_2, and X_3 all set within their respective ranges. In order to achieve the highest possible yield and minimize the maximum pressure of the system, the yield was set to its maximum value, i.e., 'maximize', while the maximum pressure of the system was set to its minimum value, i.e., 'minimize'. The boundary conditions are shown in Table 6.

According to the optimized results, when the temperature is 100 °C, the catalyst concentration is 0.77%, and the alcohol-to-alkane ratio is 4, the desired values can be achieved. At this time, the theoretical yield is 88.20%, and the maximum pressure of the system is 3.56 bar. To verify the consistency of the model with the actual results, three additional verification experiments were conducted in RC1e according to the given experimental parameters (Table 7). Taking the average of the three experimental results, we obtained an average yield of 88.58% and an average pressure of 3.62 bar, with the maximum pressure reaching 3.65 bar. The relative errors of both parameters are relatively small, which indicates that the model can accurately reflect the experimental process and can be used to predict the process results. It can serve as a reference theoretical basis for the semi-batch process production of PGME.

Analysis and study on the exothermic behavior of the PGME reaction process

Exothermic conditions of reactions under different temperature control modes

In chemical production, two commonly used temperature control modes are the isothermal mode and the isoperibolic mode. To study the thermal parameters of reactions under these two modes[26], in this work, the exothermic behavior of the reaction under isothermal and isoperibolic modes was studied under the same reaction

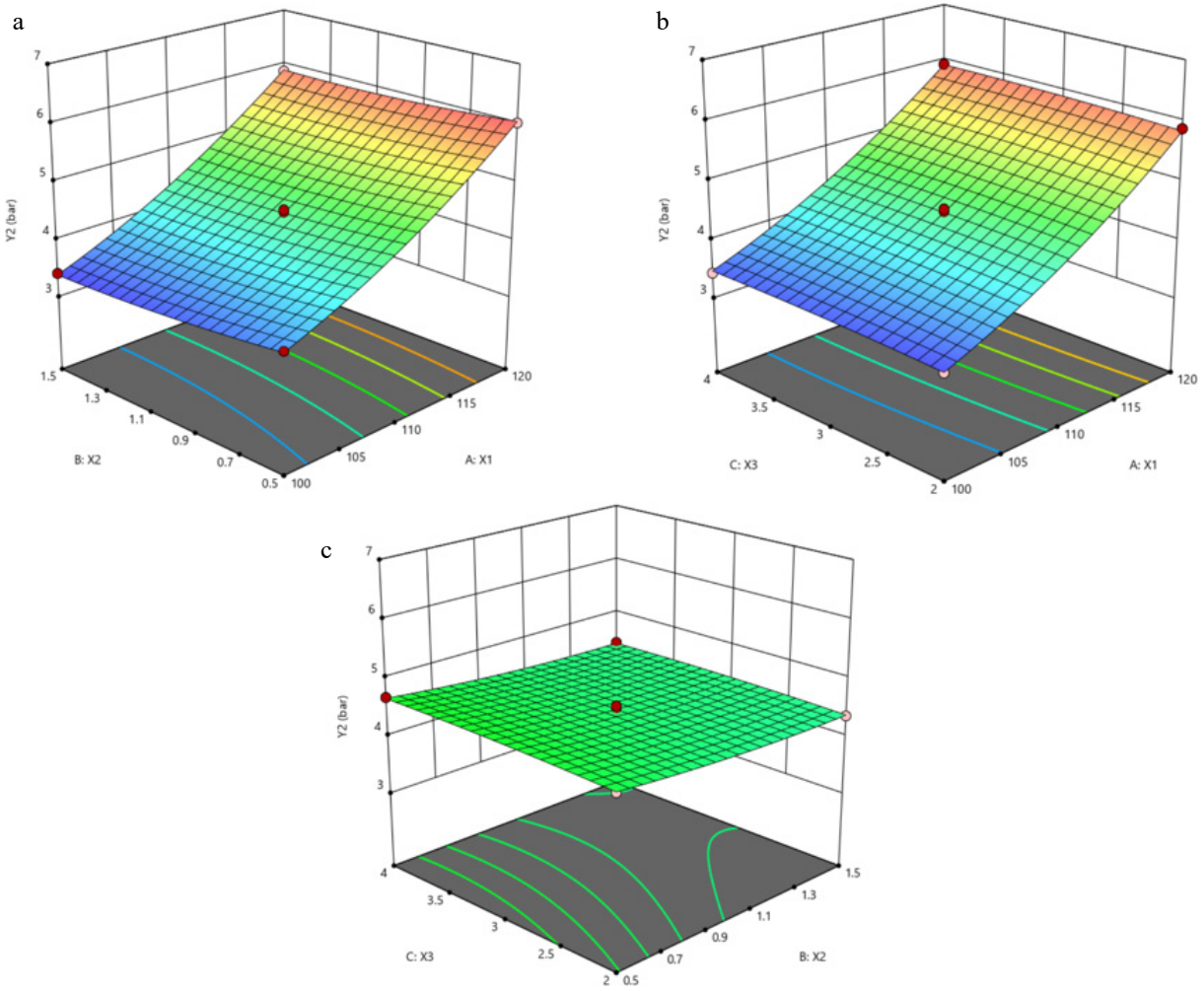

Fig. 8 Three-dimensional response diagram of the maximum pressure in the system: (a) X_1 and X_2; (b) X_1 and X_3; (c) X_2 and X_3.

https://doi.org/10.48130/emst-0026-0007

Table 6. Boundary condition settings for process optimization.

Factors and responses	Objectives	Low level	High level
X_1	In range	100	120
X_2	In range	0.5	1.5
X_3	In range	2	4
Y_1	Maximize	0	100
Y_2	Minimize	0	10

Table 7. Results of process optimization experiments.

Number	Yield of PGME (%)	Maximum pressure of the system (bar)
1	87.84	3.62
2	89.23	3.59
3	88.67	3.65
Average	88.58	3.62
Model predicted value	88.20	3.56
Relative error	0.43	1.69

parameters. The reaction temperature was set at 100 °C, the catalyst concentration at 1.5%, the ratio of PO to methanol at 1:3, and the feed rate of PO at 20 mL/min. As shown in Fig. 9, under isothermal mode, T_r reached a maximum of 104.62 °C, with a maximum temperature difference between T_r and T_j of 13.68 °C, and a maximum exothermic rate of 371.86 W. Under isoperibolic mode, the maximum temperature difference between T_r and T_j was 12.24 °C, but T_r reached a value of 112.24 °C, far exceeding the set required temperature, which would inevitably affect the yield and other results. Due to the low boiling points of the reaction raw materials, temperature had a significant impact on the system pressure. Under isoperibolic mode, T_r was higher, and the maximum system pressure was also higher than that of the former. The relevant result parameters under the two modes are shown in Table 8. It can be concluded that the isothermal mode is safer and more suitable for practical production. Therefore, the isothermal mode was adopted for subsequent reaction calorimetry experiments.

Exothermicity of reactions under different factors

The variation trends of various thermodynamic parameters during the reaction process were revealed through single-factor calorimetric experiments, as shown in Figs. 10–13.

ΔT_{ad} can be used to indicate the severity of a runaway reaction[27,28]. Since not all of the reactants are converted into the target product during the actual reaction process, it is necessary to correct it using the yield, denoted as $\Delta T_{ad,r}$, as shown in Eq. (5).

$$\Delta T_{ad} = \frac{\Delta H}{C_p M} \tag{4}$$

$$\Delta T_{ad,r} = \frac{\Delta H}{C_p M Y} \tag{5}$$

Y represents the yield, %; ΔH denotes the heat released by the reaction, kJ; C_p stands for the specific heat capacity, J/(kg·K); and M signifies the mass of material in the reaction system, kg.

MTSR refers to the maximum temperature that the system can reach when the reaction goes out of control[29,30]. The maximum value of T_{cf} is taken as *MTSR*, where T_{cf} represents the temperature reached when the accumulation of materials leads to a temperature rise in the event of cooling failure. $T_{cf,r}$ is its correction formula, and T_{cf} and $T_{cf,r}$ are calculated as follows:

$$T_{cf} = T_p + \frac{\frac{\Delta H m_t}{m} - \int_0^t qr(t)dt}{C_p M} \tag{6}$$

$$T_{cf,r} = T_p + \frac{\frac{\Delta H m_t}{mY} - \int_0^t qr(t)dt}{C_p M} \tag{7}$$

q_r represents the heat release rate, W; T_p represents the reaction temperature, °C.

ΔT_{max} represents the maximum difference between T_r and T_j. A larger difference indicates a more intense reaction and faster heat release. In this case, the heat released by the reaction causes the material temperature to increase, and the jacket temperature will drop even more in order to achieve a cooling effect.

Single-factor calorimetric experiments were designed. The experimental conditions were basically consistent with those in Table 2, and only one additional control experiment with a feeding rate of 10 mL/min was supplemented.

As shown in Fig. 10, since the reaction system consists of low-boiling-point substances, the pressure is greatly influenced by temperature. Therefore, as the temperature increases, the pressure within the system also rises. Furthermore, as the temperature continues to rise, the pressure increases approximately exponentially. When the reaction becomes uncontrollable, the continuous rise in temperature leads to a sustained increase in pressure, which ultimately results in the rupture or even explosion of the reaction device. As

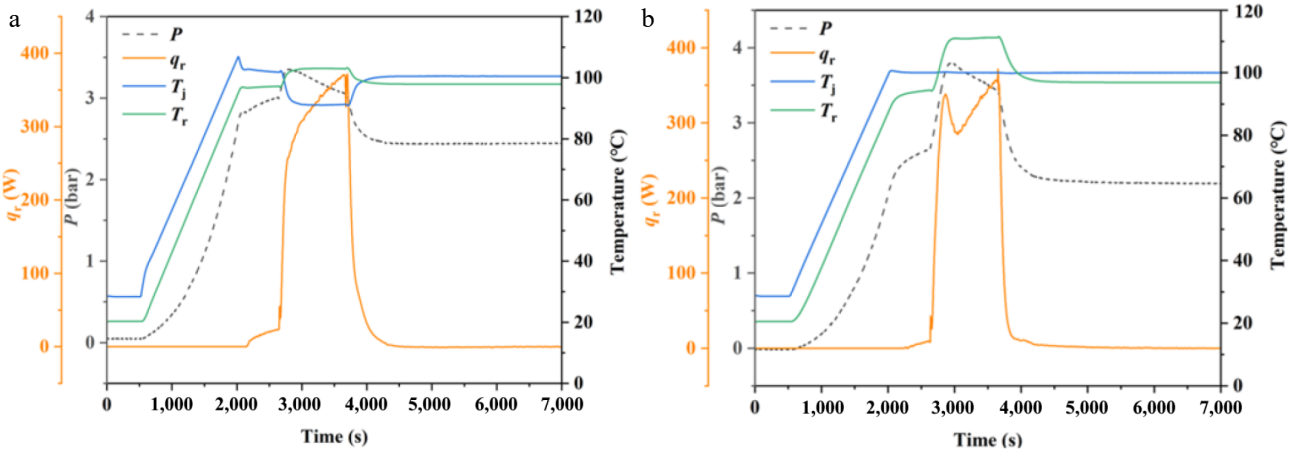

Fig. 9 Heat release behavior under different temperature control modes: (a) isothermal mode; (b) isoperibolic mode.

Table 8. Experimental parameters under different temperature control modes.

Temperature control mode	T_r (°C)	$q_{r,max}$ (W)	P_{max} (bar)	ΔH (kJ/mol)	ΔT_{max} (°C)	Total heat release (kJ)
Isothermal mode	104.62	371.86	3.41	79.25	13.68	369.9
Isoperibolic mode	112.24	371.65	3.8	71.71	12.24	334.88

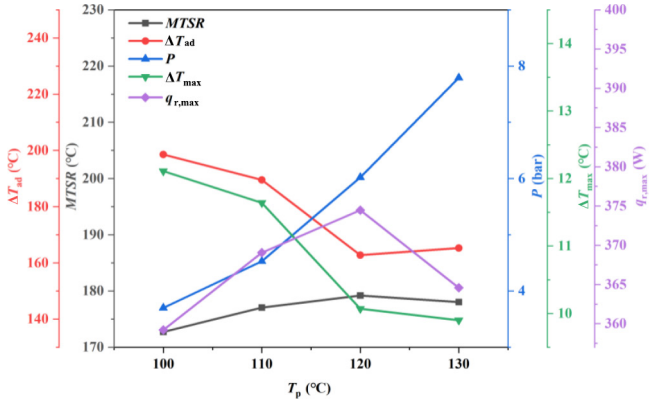

Fig. 10 Exothermic characteristics at different reaction temperatures.

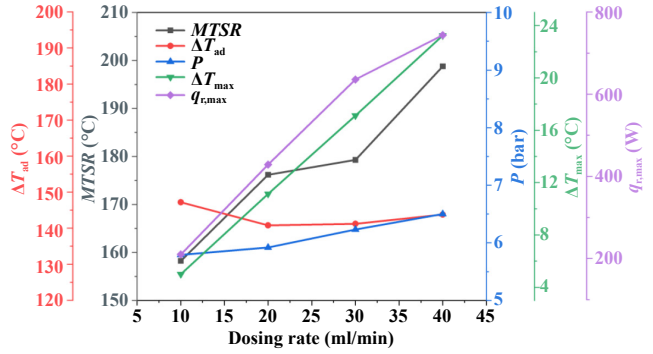

Fig. 11 Exothermic characteristics under different feeding rates.

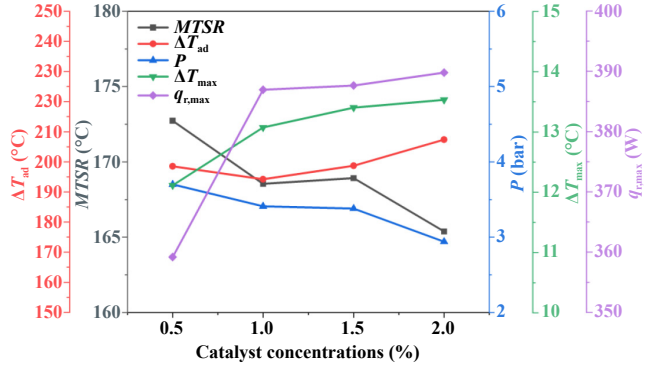

Fig. 12 Exothermic characteristics under different catalyst concentrations.

the reaction temperature continues to increase, the heat release decreases. This is because high temperature not only increases the reaction rate of the main reaction, but also accelerates the reaction rate of the side reactions. Some side reactions may release less heat than the main reaction, while occupying substances that should otherwise participate in the main reaction. According to the results measured by the gas chromatography, the yield decreases as the temperature rises, while the area of the impurity peaks increases.

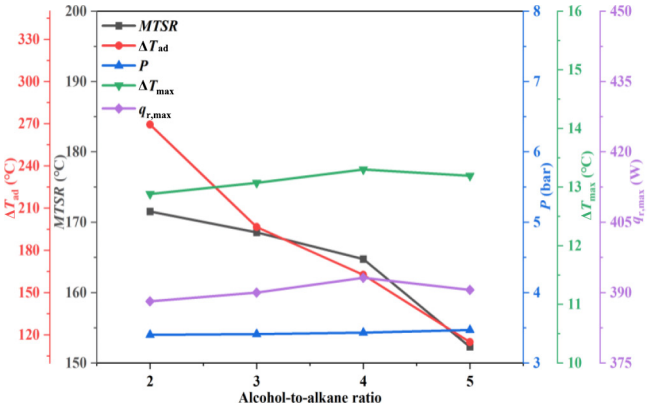

Fig. 13 Exothermic characteristics under different alcohol-to-alkane ratios.

However, the amount of PO entering the reaction kettle remains constant, ultimately leading to a continuous decrease in heat release, resulting in a continuous decrease in ΔT_{max} and ΔT_{ad}. Therefore, the reaction temperature should not be excessively high during practical production.

As shown in Fig. 11, increasing the feeding rate results in a large amount of PO entering the reaction kettle. At this time, due to the large amount of reactants in contact with the base material, the reaction proceeds more rapidly per unit time, leading to continuous increases in $q_{r,max}$, and ΔT_{max}. However, an excessively high feeding rate can increase the cumulative rate of system materials, resulting in a continuous increase in *MTSR*. Furthermore, with the continuous increase of the feeding rate, the amount of propylene oxide entering the system per unit time rises. Propylene oxide exists in both gas and liquid phases within the reactor. As the feeding rate increases, the gaseous fraction of propylene oxide accumulates, thereby leading to a notable rise in system pressure, leading to an increase in the maximum pressure of the system. Therefore, the feeding rate should be reduced as much as possible.

As shown in Fig. 12, as the catalyst concentration increases, the reaction rate accelerates, and the input PO is quickly reacted. Therefore, the amount of PO in the gas phase is consumed more rapidly, resulting in a continuous decrease in the pressure of the system, and the value of ΔT_{max} continues to rise. However, *MTSR* is greatly influenced by the degree of material accumulation. At the same reaction temperature, the higher the material accumulation degree, the higher the *MTSR*. As the catalyst concentration increases, the reaction rate increases, and the amount of PO that can be accumulated in the system decreases, so *MTSR* continues to decrease. However, the increase in catalyst input does not significantly change the amount of heat released during the reaction, so ΔT_{ad} does not change significantly. Therefore, the dosage of catalyst should not be excessively high.

As shown in Fig. 13, an increase in the alcohol-to-alkane ratio actually means reducing the amount of PO input. Since the initial reaction substrate was fixed, adjusting the alcohol-to-alkene ratio only changed the dosage of supplemented propylene oxide. This indicates that the amount of propylene oxide introduced into the reaction system per unit time remained constant. With other experimental parameters unchanged, the overall reaction rate was maintained steadily. Therefore, the values of $q_{r,max}$, ΔT_{max}, and the maximum pressure in the system remain basically unchanged. An increase in the alcohol-to-alkane ratio leads to a significant reduction in the heat released by the reaction, ΔT_{ad} decreases, and thus

https://doi.org/10.48130/emst-0026-0007

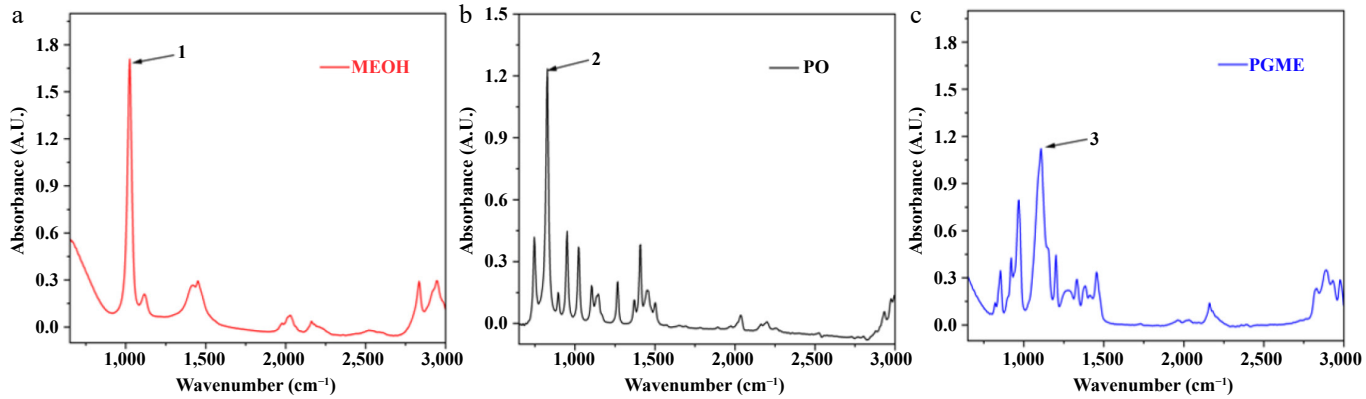

Fig. 14 Infrared spectra of samples: (a) methanol; (b) PO; (c) propylene glycol monomethyl ether.

MTSR also decreases. Therefore, in industrial production, it is necessary to increase the alcohol-to-alkane ratio for safety to control heat, but an excessively high alcohol-to-alkane ratio can also lead to increased methanol consumption, increasing production costs.

Online infrared analysis

Infrared spectroscopy analysis of substances

To conduct real-time monitoring and analysis of the reaction using online infrared spectroscopy, it is necessary to identify the characteristic peaks of the relevant substances. In this work, infrared spectroscopy analysis was performed on pure samples of the reactants methanol and PO, as well as the product propylene glycol monomethyl ether. Characteristic peaks were observed at 1,024 cm^{-1} for methanol, 828 cm^{-1} for PO, and 1,111 cm^{-1} for propylene glycol monomethyl ether, as shown in Fig. 14. Relevant information is provided in Table 9.

Exothermic reaction mechanism

Combined with online infrared real-time analysis[31], the real-time changes of substances during the reaction process can be observed. As shown in Fig. 15, the set reaction temperature is 100 °C. When PO is added to the reaction kettle near 2,600 s, the amount of propylene oxide was observed to increase. At the same time, the amount of propylene glycol monomethyl ether and the value of q_r are also continuously increasing. While the amount of methanol is decreasing, indicating that the reaction has begun, consuming methanol and PO to generate PGME while releasing heat. As the reaction continues, the heat release rate is continuously increasing. After the addition of PO is complete, the heat release rate reaches a peak, at which point the remaining PO in the kettle is still reacting. It can be observed that the increase rate of propylene glycol monomethyl ether and the consumption rate of methanol are slowing down. When the absorbances of the three characteristic peaks do not change, it indicates that the reaction has ended. At this point, it can be seen that the heat release rate is also infinitely approaching 0.

Table 9. Intense absorption peaks of substances.

Peak	Wavenumber (cm^{-1})	Functional group	Affiliation
Peak 1	1,024	C-O	MeOH
Peak 2	828	ternary monoxide ring vibration	PO
Peak 3	1,111	C-O-C	PGME

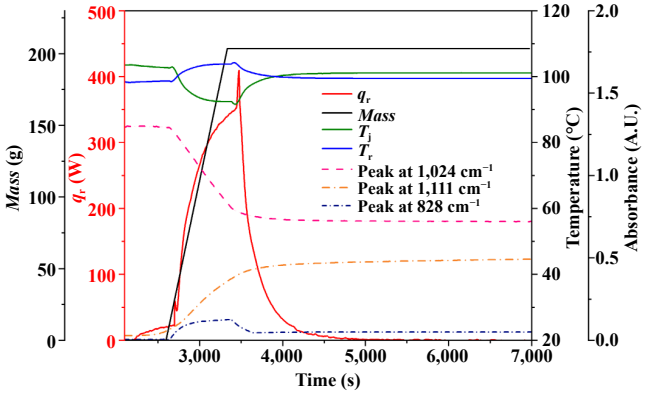

Fig. 15 Reaction process combined with online infrared spectrum.

Risk assessment of the reaction process

To assess the hazardous conditions of this reaction, it is necessary to combine the risk matrix method and Stoessel's critical graph method. In addition to the previously mentioned thermal parameters, it is also necessary to understand the *MTT* and TMR_{ad} of the reaction. Taking the optimized process as an example in this study.

MTT refers to the maximum temperature attainable due to technical reasons, which is determined by the pressure conditions of the reaction system and the boiling point of the materials. Since this reaction is conducted in an autoclave, the *MTT* should be determined as the temperature corresponding to the maximum pressure during the reaction process. Given that methanol accounts for the largest proportion in the system, methanol is selected for calculation. The Antoine Equation is used to calculate the *MTT* at a maximum pressure of 3.54 bar, which is 102.2 °C. The Antoine Equation is shown in Eq. (8):

$$\log P = A - \frac{B}{t + C} \tag{8}$$

Here, *P* refers to pressure, t stands for temperature, and *A*, *B*, and *C* are constants.

TMR_{ad} represents the time required to achieve the maximum reaction rate under the condition of no heat exchange, while T_{D24} denotes the temperature of TMR_{ad} at 24 h. Immediate testing of the product after the reaction using an accelerated adiabatic calorimeter revealed no exothermic phenomenon (heating up to 350 °C). A total of 0.58 g of the product was taken for the experiment. The experimental result is shown in Fig. 16, indicating that the product does not exhibit exothermic decomposition characteristics. The thermal hazard of the product is relatively low, and it can be

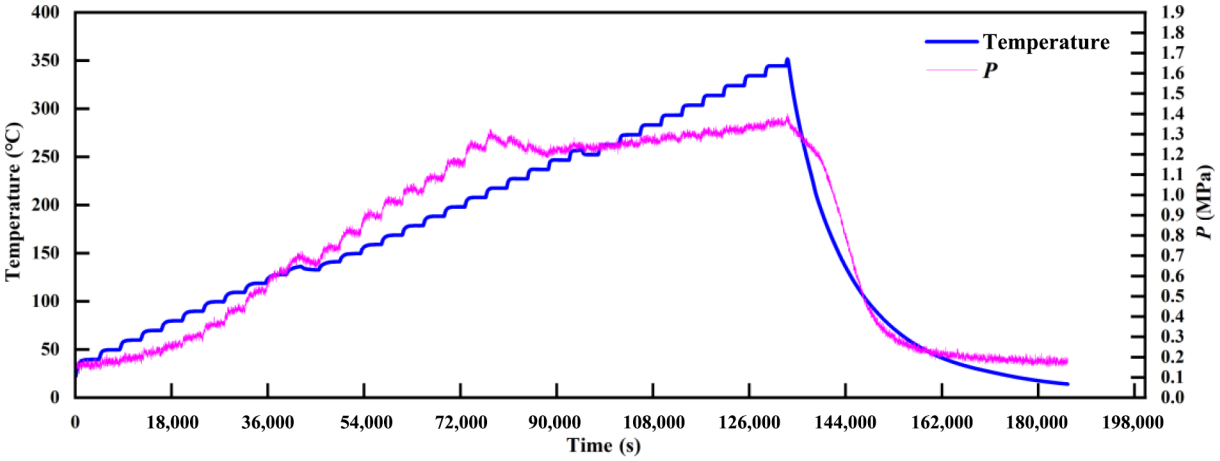

Fig. 16 The adiabatic calorimetric diagram of the product.

Table 10. Results of the risk matrix assessment.

$\Delta T_{ad,r}$ (°C)	Severity	TMR_{ad} (h)	Possibility	Risk level
158.47	marginal	> 24	negligible	1

Table 11. Response risk level assessment.

T_p (°C)	$MTSR_r$ (°C)	MTT (°C)	T_{D24} (°C)	Class
100	162.2	102.2	> 350	3

confirmed that T_{D24} is greater than 350 °C, making the likelihood of secondary decomposition triggered by the product in the event of thermal runaway relatively low.

Using the risk matrix, the severity ($\Delta T_{ad,r}$) and probability (TMR_{ad}) are combined to determine the risk level. As shown in Table 10, through calculation, the value of $\Delta T_{ad,r}$ is found to be 158.47 K, with the severity of the out-of-control reaction being classified as Level 2. Since TMR_{ad} is greater than 24, the probability of the reaction going out of control is classified as Level 1. Comprehensively evaluated, the acceptability of the out-of-control reaction is classified as Level 1, indicating that the risk is acceptable. Furthermore, using the Stoessel assessment method to evaluate the risk level of the reaction cooling failure, as shown in Table 11, it can be found that the critical level of this reaction is Level 3. This indicates that there is a potential risk of material boiling leading to material surge ($MTSR_r > MTT$), but the probability of triggering a secondary decomposition reaction is not high ($T_{D24} > MTSR_r$). Therefore, for this reaction, it is necessary to fully consider implementing emergency decompression and emergency cooling risk control measures to avoid material surge and the potential secondary risks that could lead to explosion accidents.

Conclusions

In this study, the working curves of PGME and PO were first plotted. Subsequently, the reaction path and reaction enthalpy were calculated based on DFT, yielding a heat release of approximately 85.41 kJ/mol for this reaction. Experimental measurements were further conducted using the RC1e reaction calorimeter, and the obtained result was 84.95 kJ/mol, which is in good agreement with the theoretical value. The single-factor method was then adopted to analyze the yield and maximum system pressure in the process of preparing PGME from PO, which identified the suitable ranges for reaction temperature, catalyst concentration, and alcohol-to-alkane ratio. Based on these ranges, the RSM was utilized to optimize the reaction yield and pressure. The results showed that the yield reached 88.20% when the reaction temperature was 100 °C, the alcohol-to-alkane ratio was 4, and the catalyst concentration was 0.77%. Simultaneously, the pressure could be reduced to 3.56 bar. Three sets of experiments were conducted to verify the results, and the error of the results is less than 2%, demonstrating the rationality of the model. Subsequently, calorimetric experiments were performed to investigate the changes in reaction-related parameters under different factors. In addition, *in-situ* infrared spectroscopy was used to study the changes of various substances and thermal behavior during the reaction process. Accelerating Rate Calorimeter experiments on the products indicated no decomposition. The risk level of the reaction was determined to be acceptable using the risk matrix method, and the reaction was assessed as a third-order reaction based on the Stoessel critical diagram. The reaction posed a certain degree of danger, necessitating strict control of the feeding rate and consideration of emergency decompression measures to avoid material rush and explosion risks.

Author contributions

The authors confirm their contributions to the paper as follows: overall conception and design of the research: Ni L, Fang X, Cheng Z; provision of resources: Ni L; data collection, processing and paper writing: Fang X, Li N; review of the results, revision and approvement of the final version of the manuscript: Ni L, Fang X, Li N, Cheng Z, Chen Z, Li Z. All authors reviewed the results and approved the final version of the manuscript.

Data availability

All data generated or analyzed during this study are included in this published article.

Acknowledgments

This work appreciates the support of National Natural Science Foundation of China (Nos. 52274209, 52334006, and 52304229).

Conflict of interest

The authors declare that they have no conflict of interest.

https://doi.org/10.48130/emst-0026-0007

Dates

Received 14 April 2026; Revised 6 May 2026; Accepted 9 May 2026; Published online 31 July 2026

References

[1] Wang Z, Zhang A, Zhu M, Lin C, Chen X, et al. 2025. Regulating the hydrophilicity and complexation of poly(pyrrole methane) by phenolic hydroxyl groups for efficient Mercury(II) capture. *Separation and Purification Technology* 354:128712

[2] Hopf NB, Vernez D, Berthet A, Charriere N, Arnoux C, et al. 2012. Effect of age on toxicokinetics among human volunteers exposed to propylene glycol methyl ether (PGME). *Toxicology Letters* 211:77–84

[3] Spencer PJ. 2005. New toxicity data for the propylene glycol ethers – a commitment to public health and safety. *Toxicology Letters* 156:181–188

[4] Timofeeva MN, Panchenko VN, Jun JW, Hasan Z, Kikhtyanin OV, et al. 2013. Effect of the acid–base properties of metal phosphate molecular sieves on the catalytic performances in synthesis of propylene glycol methyl ether from methanol and propylene oxide. *Microporous and Mesoporous Materials* 165:84–91

[5] Chitwood HC, Freure BT. 1946. The reaction of propylene oxide with alcohols. *Journal of the American Chemical Society* 68: 680–683

[6] Timofeeva MN, Paukshtis EA, Panchenko VN, Shefer KI, Isaeva VI, et al. 2019. Tuning the catalytic performance of novel composites based on ZIF-8 and nafen through dimensional and concentration effects in the synthesis of propylene glycol methyl ether. *European Journal of Organic Chemistry* 2019:4215–4225

[7] Zhao C, Chen S, Zhang R, Li Z, Liu R, et al. 2017. Synthesis of propylene glycol ethers from propylene oxide catalyzed by environmentally friendly ionic liquids. *Chinese Journal of Catalysis* 38:879–888

[8] Timofeeva MN, Panchenko VN, Gil A, Chesalov YA, Sorokina TP, et al. 2011. Synthesis of propylene glycol methyl ether from methanol and propylene oxide over alumina-pillared clays. *Applied Catalysis B: Environmental* 102:433–440

[9] Rupp M, Ruback W, Klemm E. 2013. Octanol ethoxylation in microchannels. *Chemical Engineering and Processing: Process Intensification* 74:19–26

[10] Gustin JL. 2005. Understanding vinyl acetate polymerization accidents. *Chemical Health & Safety* 12:36–46

[11] Lin CP, Li JS, Tseng JM, Mannan MS. 2016. Thermal runaway reaction for highly exothermic material in safe storage temperature. *Journal of Loss Prevention in the Process Industries* 40:259–265

[12] Bou-Diab L, Fierz H. 2002. Autocatalytic decomposition reactions, hazards and detection. *Journal of Hazardous Materials* 93:137–146

[13] Stoessel F. 2008. Assessment of thermal risks. In *Thermal Safety of Chemical Processes: Risk Assessment and Process Design*. USA: Wiley. pp. 59–80. doi: 10.1002/9783527621606.ch3

[14] Xu C, Zhang M, Zhang Y, Hu J, Bi F, et al. 2025. Thermal decomposition behavior and safety assessment of Diazidoglyoxime (DAzG) synthesis for TKX-50 production: a calorimetric and risk classification study. *FirePhysChem* 5:558–570

[15] Jiang J, Jiang W, Ni L, Zhang W, Zou M, et al. 2019. The modified Stoessel criticality diagram for process safety assessment. *Process Safety and Environmental Protection* 129:112–118

[16] Berdouzi F, Villemur C, Olivier-Maget N, Gabas N. 2018. Dynamic simulation for risk analysis: application to an exothermic reaction. *Process Safety and Environmental Protection* 113:149–163

[17] Wang SY, Kossoy AA, Yao YD, Chen LP, Chen WH. 2017. Kinetics-based simulation approach to evaluate thermal hazards of benzaldehyde oxime by DSC tests. *Thermochimica Acta* 655:319–325

[18] Yu A, Zhou J, Hua M, Pan X, Jiang J, et al. 2023. Predicting thermal runaway in styrene polymerization reactions: divergence criterion with phase space reconstruction. *Process Safety and Environmental Protection* 172:802–814

[19] Chen KY, Wu SH, Wang YW, Shu CM. 2008. Runaway reaction and thermal hazards simulation of cumene hydroperoxide by DSC. *Journal of Loss Prevention in the Process Industries* 21:101–109

[20] Lu KT, Luo KM, Lin SH, Su SH, Hu KH. 2004. The acid-catalyzed phenol–formaldehyde reaction: critical runaway conditions and stability criterion. *Process Safety and Environmental Protection* 82:37–47

[21] Hiltz JA. 2015. Analytical pyrolysis gas chromatography/mass spectrometry (py-GC/MS) of poly(ether urethane)s, poly(ether urea)s and poly(ether urethane-urea)s. *Journal of Analytical and Applied Pyrolysis* 113:248–258

[22] Merayo N, Hermosilla D, Cortijo L, Blanco Á. 2014. Optimization of the Fenton treatment of 1, 4-dioxane and on-line FTIR monitoring of the reaction. *Journal of Hazardous Materials* 268:102–109

[23] Parker T, Mao Y, Wang Q. 2022. Application of response surface methodology for hazard analysis of 2-butanol oxidation to 2-butanone using RC1 calorimetry. *Journal of Loss Prevention in the Process Industries* 75:104703

[24] Pereda-Ayo B, Duraiswami D, González-Marcos JA, González-Velasco JR. 2011. Performance of NO_x storage–reduction catalyst in the temperature–reductant concentration domain by response surface methodology. *Chemical Engineering Journal* 169:58–67

[25] Sinaei Nobandegani M, Sardashti Birjandi MR, Darbandi T, Khalilipour MM, Shahraki F, et al. 2016. An industrial Steam Methane Reformer optimization using response surface methodology. *Journal of Natural Gas Science and Engineering* 36:540–549

[26] Salcedo WNV, Mignot M, Renou B, Leveneur S. 2023. Assessment of kinetic models for the production of γ-valerolactone developed in isothermal, adiabatic and isoperibolic conditions. *Fuel* 350:128792

[27] Das PK. 2012. Theoretical estimation of adiabatic temperature rise from the heat flow data obtained from a reaction calorimeter. *Thermochimica Acta* 530:17–24

[28] Hada S, Harrison BK. 2007. Prediction of energy release hazards using a simplified adiabatic temperature rise. *Journal of Loss Prevention in the Process Industries* 20:151–157

[29] Chen LP, Liu TT, Yang Q, Chen WH. 2012. Thermal hazard evaluation for iso-octanol nitration with mixed acid. *Journal of Loss Prevention in the Process Industries* 25:631–635

[30] Lerena P, Wehner W, Weber H, Stoessel F. 1996. Assessment of hazards linked to accumulation in semi-batch reactors. *Thermochimica Acta* 289:127–142

[31] Hovorun DM, Voiteshenko IS, Gorb L. 2023. Manifestations of intramolecular H-bonds of CH… O and OH… C type in quercetin molecule: analysis of IR spectra by mean of density functional theory. *Spectrochimica Acta Part A: Molecular and Biomolecular Spectroscopy* 287:122065